

Analysis of a Three-Phase Twelve-Pulse Voltage Output Type Rectifier

Predrag Pejović and Johann W. Kolar

Abstract—Exact solution of a circuit model for a three-phase twelve-pulse rectifier with constant-voltage load and ac-side reactance for the continuous conduction mode is presented. Obtained results are compared to the results provided by sinusoidal approximation. It is shown that the sinusoidal approximation provides acceptable results at low output voltages, with the accuracy being decreased for the output voltages approaching to the discontinuous conduction mode boundary. In comparison to the exact solution, the sinusoidal approximation always provides slightly more optimistic prediction for the rectifier exploitation parameters. Computational complexity of the exact solution is the same as for the solution obtained applying sinusoidal approximation, having the same structure, but different parameters. In comparison to the six-pulse rectifiers of the same type, analyzed in previous publications, agreement between the solutions is better due to the increased pulse number and reduced harmonic content of the waveforms.

Index Terms—AC-DC power conversion, converters, harmonic distortion, power conversion harmonics, power quality, rectifiers.

I. INTRODUCTION

IN this paper, the rectifier presented in Fig. 1 is analyzed in order to obtain closed form analytical expressions for its performance parameters, like the dependence of the output voltage on the output current, dependence of the input current THD on the output voltage, maximum of the output power the rectifier might provide, etc. The rectifier is proposed in [1], and it consists of two three-phase diode bridges, filtering capacitor, three coupling inductors, and a line-side interphase transformer. Construction of the rectifier is simple and robust, without controlled switches, high frequency switching, and related problems of electromagnetic interference, increased losses, and reliability issues. This makes the design suitable for application in harsh environments and in cases where low maintenance and high reliability are required. Basic version of the rectifier, proposed in [1] and shown in Fig. 1, provides twelve-pulse voltage waveforms v_{Tk} , $k \in \{1, 2, 3\}$, at the inputs of the line-side interphase transformer, that are coupled to the mains by three inductors. In comparison to the current output type rectifiers, the coupling inductors are used instead of the filtering inductor at the dc side.

The basic structure of the rectifier is extended in [2], [3] to provide 18-pulse operation and recuperation [2]. An analysis of the rectifier operating principles is presented in [4], as well as an extension of the structure to provide 24-pulse operation. In [5], harmonic cancellation approach is applied in the analysis of the line-side interphase transformer, and controlled switches are applied to provide 24-pulse operation.

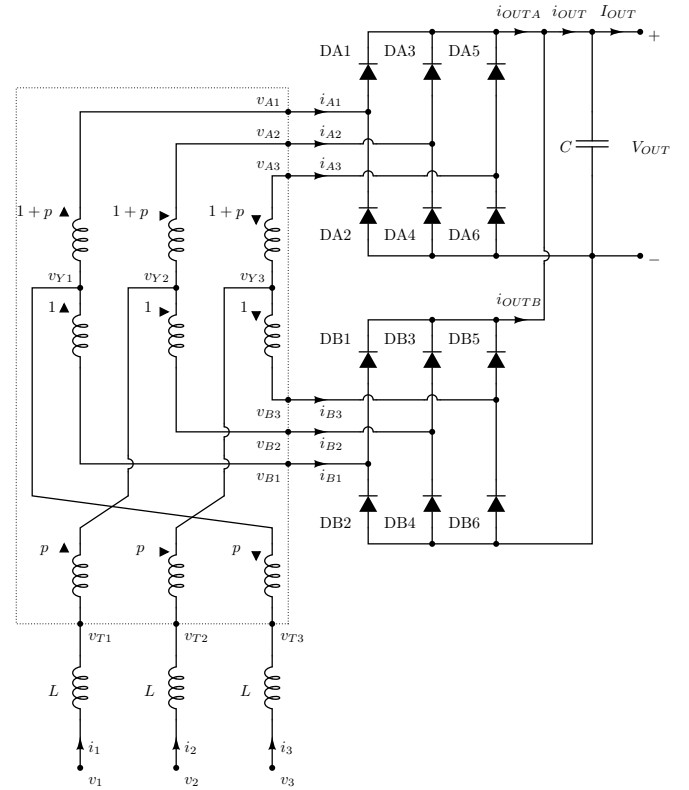


Fig. 1. The rectifier.

Although three-phase voltage output type rectifiers have simple structure, their analysis is not straightforward. In [6], sinusoidal approximation is applied to analyze the six-pulse version of the rectifier while it operates in the continuous conduction mode. Performance parameters of the rectifier are derived, as well as the output voltage range where the rectifier operates in the continuous conduction mode. In the case the rectifier losses are negligible, the exact solution for the continuous conduction mode is presented in [7]. The exact solution has the same computation complexity as the solution obtained applying sinusoidal approximation, but provides additional information about the performance parameters, like the input current THD and the difference between the power factor and the displacement power factor.

Aim of the research presented in this paper is to provide a closed-form analytical solution for the rectifier of Fig. 1 while it operates in the continuous conduction mode. The continuous conduction mode is characterized by absence of the intervals when some of the input currents of the diode bridges are equal to zero. In the continuous conduction mode,

in each of the diode bridges, and in each time point, three of the diodes are conducting. The first step in the analysis is the sinusoidal approximation approach, which provides a good starting point to obtain the exact solution and some directly applicable intermediate results. Methods applied to obtain the exact solution are somewhat more complex than in [7], due to increased complexity of the structure caused by the line-side interphase transformer.

The line-side interphase transformer is applied to split the input currents and to provide equal load sharing between the two diode bridges. Besides, it provides appropriate phase shift to form twelve-pulse input voltages of the line-side interphase transformer v_{T1} , v_{T2} , and v_{T3} on the basis of its output voltages v_{A1} , v_{A2} , v_{A3} , v_{B1} , v_{B2} , and v_{B3} . The line-side interphase transformer is assumed to be built using three single-phase ferromagnetic cores, which results in negligible magnetizing currents. Another option that provides low magnetizing currents is application of a shell type three-phase core or a five-limb core, with a huge magnetizing inductance for the zero-sequence component. Under these assumptions, assuming perfect magnetic coupling further, the line-side interphase transformer is characterized by

$$i_{A1} = \frac{1}{p+2}i_1 - \frac{p}{p+2}i_2 \quad (1)$$

$$i_{A2} = \frac{1}{p+2}i_2 - \frac{p}{p+2}i_3 \quad (2)$$

$$i_{A3} = \frac{1}{p+2}i_3 - \frac{p}{p+2}i_1 \quad (3)$$

$$i_{B1} = \frac{p+1}{p+2}i_1 + \frac{p}{p+2}i_2 \quad (4)$$

$$i_{B2} = \frac{p+1}{p+2}i_2 + \frac{p}{p+2}i_3 \quad (5)$$

$$i_{B3} = \frac{p+1}{p+2}i_3 + \frac{p}{p+2}i_1 \quad (6)$$

$$v_{T1} = \frac{1}{p+2}v_{A1} + \frac{p+1}{p+2}v_{B1} - \frac{p}{p+2}(v_{A3} - v_{B3}) \quad (7)$$

$$v_{T2} = \frac{1}{p+2}v_{A2} + \frac{p+1}{p+2}v_{B2} - \frac{p}{p+2}(v_{A1} - v_{B1}) \quad (8)$$

and

$$v_{T3} = \frac{1}{p+2}v_{A3} + \frac{p+1}{p+2}v_{B3} - \frac{p}{p+2}(v_{A2} - v_{B2}). \quad (9)$$

To provide proper phase shift and twelve-pulse waveforms of v_{Tk} , $k \in \{1, 2, 3\}$, the turns ratio parameter should be set to

$$p = \frac{\sqrt{3}-1}{2} \approx 0.366 \quad (10)$$

according to [1].

In the analyses that follow, the rectifier would be assumed to be supplied by a symmetric undistorted three-phase voltage system

$$v_k = V_m \sin\left(\omega t - (k-1)\frac{2\pi}{3}\right) \quad (11)$$

for $k \in \{1, 2, 3\}$, where V_m is the phase voltage amplitude.

To simplify the analysis and to generalize the results, normalization of voltages, currents, and time are performed in the same manner as in [7], replacing voltages with their normalized equivalents according to

$$m = \frac{1}{V_m} v \quad (12)$$

while the currents are normalized applying

$$j = \frac{\omega L}{V_m} i. \quad (13)$$

The time variable is replaced by the phase angle equivalent

$$\varphi = \omega t. \quad (14)$$

After the normalization is performed, governing equations for the inductor currents are transformed from

$$L \frac{di_k}{dt} = v_k - v_{Tk} \quad (15)$$

to

$$\frac{dj_k}{d\varphi} = m_k - m_{Tk}. \quad (16)$$

Aim of the analysis is to obtain the steady-state response, with all the voltages and currents periodic with the period of 2π in phase angle.

To determine waveforms of the rectifier voltages, it is important to note that the input voltages are free from the zero-sequence component, according to (11), thus

$$v_1 + v_2 + v_3 = 0. \quad (17)$$

Since the rectifier is connected as a three-wire system,

$$i_1 + i_2 + i_3 = 0. \quad (18)$$

Voltages at the line-side interphase transformer input terminals are given by

$$v_{Tk} = v_k - L \frac{di_k}{dt} \quad (19)$$

for $k \in \{1, 2, 3\}$. According to (17) and (18), this results in

$$v_{T1} + v_{T2} + v_{T3} = 0. \quad (20)$$

In the analysis, the output capacitor is assumed to be large enough to provide constant output voltage

$$V_{OUT} = v_{OUTP} - v_{OUTM}. \quad (21)$$

Equations (20) and (21) are essential in obtaining waveforms of the rectifier voltages.

II. SINUSOIDAL APPROXIMATION

The sinusoidal approximation in the analysis of the rectifier of Fig. 1 is based upon the assumption that the inductor currents are sinusoidal, given by

$$i_k = I_{m1} \sin\left(\omega t - \phi - (k-1)\frac{2\pi}{3}\right) \quad (22)$$

for $k \in \{1, 2, 3\}$, which takes normalized form

$$j_k = J_{m1} \sin\left(\varphi - \phi - (k-1)\frac{2\pi}{3}\right). \quad (23)$$

The currents of the inductors are assumed to have the same amplitude, being mutually shifted in phase for $2\pi/3$, due to symmetry. Each of the inductor currents is assumed to be delayed in phase for ϕ in regard to the corresponding phase voltage.

Assumed input currents specify the line-side interphase transformer output currents according to (1)–(6) and (10), resulting in their normalized waveforms

$$j_{Ak} = \frac{\sqrt{3}-1}{\sqrt{2}} J_{m1} \sin\left(\varphi - \phi + \frac{\pi}{12} - (k-1)\frac{2\pi}{3}\right) \quad (24)$$

and

$$j_{Bk} = \frac{\sqrt{3}-1}{\sqrt{2}} J_{m1} \sin\left(\varphi - \phi - \frac{\pi}{12} - (k-1)\frac{2\pi}{3}\right). \quad (25)$$

The line side interphase transformer output currents determine states of the diodes in the diode bridges, such that

$$DA_{2k-1} = \begin{cases} 1, & i_{Ak} > 0 \\ 0, & i_{Ak} < 0 \end{cases} \quad (26)$$

$$DA_{2k} = 1 - DA_{2k-1} = \begin{cases} 1, & i_{Ak} < 0 \\ 0, & i_{Ak} > 0 \end{cases} \quad (27)$$

$$DB_{2k-1} = \begin{cases} 1, & i_{Bk} > 0 \\ 0, & i_{Bk} < 0 \end{cases} \quad (28)$$

and

$$DB_{2k} = 1 - DB_{2k-1} = \begin{cases} 1, & i_{Bk} < 0 \\ 0, & i_{Bk} > 0 \end{cases} \quad (29)$$

for $k \in \{1, 2, 3\}$. At this point, it is convenient to define variables that contain numbers of conducting diodes

$$DA_{UP} = DA_1 + DA_3 + DA_5 \quad (30)$$

$$DA_{DN} = DA_2 + DA_4 + DA_6 \quad (31)$$

$$DB_{UP} = DB_1 + DB_3 + DB_5 \quad (32)$$

and

$$DB_{DN} = DB_2 + DB_4 + DB_6. \quad (33)$$

In the continuous conduction mode, these variables can take only two values, 1 or 2, and they are constrained by the fact that in the continuous conduction mode in each time point three diodes are conducting in each of the diode bridges

$$DA_{UP} + DA_{DN} = 3 \quad (34)$$

and

$$DB_{UP} + DB_{DN} = 3. \quad (35)$$

States of the diodes determine voltages of the line-side interphase transformer output terminals according to

$$m_{Ak} = DA_{2k-1}m_{OUTP} + DA_{2k}m_{OUTM} \quad (36)$$

and

$$m_{Bk} = DB_{2k-1}m_{OUTP} + DB_{2k}m_{OUTM} \quad (37)$$

TABLE I
VALUES OF THE RECTIFIER OUTPUT TERMINAL VOLTAGES

DA_{UP}	DA_{DN}	m_{OUTP}	m_{OUTM}
1	1	$\frac{2}{3}M_{OUT}$	$-\frac{1}{3}M_{OUT}$
1	2	$\frac{3-\sqrt{3}}{3}M_{OUT}$	$-\frac{\sqrt{3}}{3}M_{OUT}$
2	1	$\frac{\sqrt{3}}{3}M_{OUT}$	$-\frac{3-\sqrt{3}}{3}M_{OUT}$
2	2	$\frac{1}{3}M_{OUT}$	$-\frac{2}{3}M_{OUT}$

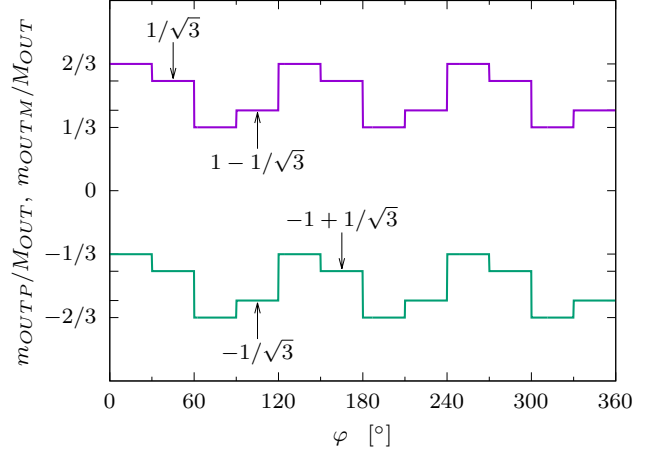


Fig. 2. Waveforms of m_{OUTP} and m_{OUTM} normalized to M_{OUT} for $\phi = 45^\circ$.

for $k \in \{1, 2, 3\}$. At this point, values of m_{OUTP} and m_{OUTM} are not known. However, these values can be determined solving the system derived from (20) and (21)

$$\begin{aligned} & ((2 - \sqrt{3}) DA_{UP} + (\sqrt{3} - 1) DB_{UP}) m_{OUTP} + \\ & + ((2 - \sqrt{3}) DA_{DN} + (\sqrt{3} - 1) DB_{DN}) m_{OUTM} = 0 \end{aligned} \quad (38)$$

and

$$m_{OUTP} - m_{OUTM} = M_{OUT}. \quad (39)$$

According to the constraints imposed to the values DA_{UP} , DA_{DN} , DB_{UP} , and DB_{DN} can take, and their mutual dependence given by (34) and (35), there are four distinct solutions of the equation system (38) and (39), as given in Table I. The waveforms of m_{OUTP} and m_{OUTM} corresponding to the currents specified by (23) are shown in Fig. 2. After m_{OUTP} and m_{OUTM} are obtained, waveforms of m_{Ak} and m_{Bk} are determined by (36) and (37) for $k \in \{1, 2, 3\}$. Finally, the waveforms of m_{Tk} are obtained applying (7)–(9). The waveform of m_{T1} is shown in Fig. 3.

States of the diodes (26)–(29) are determined only by signs of the currents i_{Ak} and i_{Bk} , $k \in \{1, 2, 3\}$. Thus, the results (30)–(39) are applicable in all situations where the rectifier operates in the continuous conduction mode, not only when the sinusoidal approximation is applied.

The waveforms of the line-side interphase transformer input

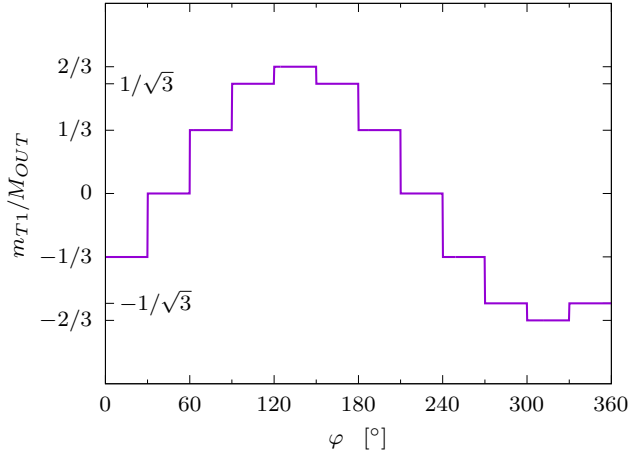


Fig. 3. Waveform of m_{T1} normalized to M_{OUT} for $\phi = 45^\circ$.

voltages are in the sinusoidal approximation represented by their fundamental harmonic, $m_{Tk,1}$,

$$m_{Tk,1} = M_{Tm1} \sin\left(\varphi - \phi - (k-1)\frac{2\pi}{3}\right) \quad (40)$$

for $k \in \{1, 2, 3\}$, where the amplitude of the fundamental harmonic is

$$M_{Tm1} = \frac{2}{\pi} (\sqrt{6} - \sqrt{2}) M_{OUT}. \quad (41)$$

Complete expansion of m_{Tk} in Fourier series provides spectrum that has nonzero harmonic components of the order $12n \pm 1$, for $n \in N$, with the amplitudes

$$M_{Tm(12n \pm 1)} = \frac{2}{\pi} (\sqrt{6} - \sqrt{2}) \frac{(-1)^n}{12n \pm 1} M_{OUT}. \quad (42)$$

According to (23) and (40), the fundamental harmonics of v_{Tk} are in phase with the corresponding phase currents, and they are mutually related by the emulated resistance, $v_{Tk,1} = R_E i_k$, i.e. $m_{Tk,1} = \rho_E j_k$ in normalized form, where

$$\rho_E = \frac{R_E}{\omega L} = \frac{M_{Tm1}}{J_{m1}} = \frac{24}{\pi^2} (2 - \sqrt{3}) \frac{M_{OUT}}{J_{OUT}} \quad (43)$$

is normalized value of the emulated resistance. This results in the phasor diagram shown in Fig. 4, which is used to determine amplitude of the input current for a given value of the output voltage. Since $|\vec{M}_k| = 1$, $|\vec{M}_{Tk,1}| = M_{Tm1}$, and $|\vec{M}_{Lk}| = |\vec{J}_k| = J_{m1}$ due to normalization, the amplitude of the input current is obtained as

$$J_{m1} = \sqrt{1 - M_{Tm1}^2}. \quad (44)$$

After the input current amplitude is determined, application of (1)–(6) provides amplitudes of the diode bridge input currents as

$$J_{Am1} = J_{Bm1} = \frac{\sqrt{3} - 1}{\sqrt{2}} J_{m1}. \quad (45)$$

Since there are two diode bridges, according to [6] the output current is obtained as

$$J_{OUT} = \frac{6}{\pi} J_{Am1} = \frac{3}{\pi} (\sqrt{6} - \sqrt{2}) J_{m1}. \quad (46)$$

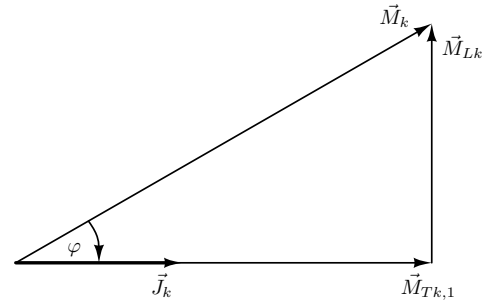


Fig. 4. The phasor diagram.

Applying (41) and (46) in (44), the output variables are related as

$$\begin{aligned} J_{OUT} &= \frac{3(\sqrt{6} - \sqrt{2})}{\pi} \sqrt{1 - (2 - \sqrt{3}) \left(\frac{4}{\pi} M_{OUT}\right)^2} \\ &\approx 0.9886 \sqrt{1 - 0.4344 M_{OUT}^2}. \end{aligned} \quad (47)$$

In practice, it is convenient to have this equation in its inverted form

$$\begin{aligned} M_{OUT} &= \frac{\pi(\sqrt{6} + \sqrt{2})}{8} \sqrt{1 - (2 + \sqrt{3}) \left(\frac{\pi}{6} J_{OUT}\right)^2} \\ &\approx 1.5173 \sqrt{1 - 1.0232 J_{OUT}^2}. \end{aligned} \quad (48)$$

Normalized output power is given by

$$\begin{aligned} P_{OUT} &= \\ &= \frac{3(\sqrt{6} - \sqrt{2})}{\pi} M_{OUT} \sqrt{1 - (2 - \sqrt{3}) \left(\frac{4}{\pi} M_{OUT}\right)^2}. \end{aligned} \quad (49)$$

The output power reaches maximum when

$$\frac{dP_{OUT}}{dM_{OUT}} = 0 \quad (50)$$

at

$$M_{OUT} = (\sqrt{3} + 1) \frac{\pi}{8} \approx 1.0729. \quad (51)$$

The maximum of normalized output power is

$$P_{OUTmax} = \frac{3}{4} = 0.75 \quad (52)$$

which is one half of the short circuit apparent power.

Since the input currents are assumed sinusoidal, the power factor and the displacement power factor are the same, which is according to the phasor diagram of Fig. 4 equal to the normalized amplitude of the line-side interphase transformer input voltage fundamental harmonic,

$$PF = DPF = M_{Tm1} = \frac{2}{\pi} (\sqrt{6} - \sqrt{2}) M_{OUT}. \quad (53)$$

The sinusoidal approximation excludes the discontinuous conduction mode, since the input currents, and consequently the input currents of the diode bridges, are assumed sinusoidal, continuously flowing in time. However, occurrence of the discontinuous conduction mode can be predicted applying sinusoidal approximation, since the continuous conduction

requires currents j_{Ak} and j_{Bk} to continue to flow after the zero crossing and thus related commutation. In the case of j_{A1} and j_{B1} , this reduces to

$$\left. \frac{dj_{A1}}{d\varphi} \right|_{-\frac{\pi}{12} + \phi^+} > 0 \quad (54)$$

and

$$\left. \frac{dj_{B1}}{d\varphi} \right|_{\frac{\pi}{12} + \phi^+} > 0. \quad (55)$$

The derivatives of the line-side interphase transformer output currents should be obtained from (1)–(6) and the inductor equations (16). In the example of j_{Ak} currents, this reduces to

$$\begin{aligned} \frac{dj_{A1}}{d\varphi} &= \frac{1}{p+2} \frac{dj_1}{d\varphi} - \frac{p}{p+2} \frac{dj_2}{d\varphi} = \\ &= \frac{1}{p+2} (m_1 - m_{T1}) - \frac{p}{p+2} (m_2 - m_{T2}). \end{aligned} \quad (56)$$

Appropriate voltage values according to the required phase angle should be used. Twelve inequalities of this kind can be written, and each of them provides the same condition for the continuous conduction mode operation

$$M_{OUT} < M_{OUTmax} \quad (57)$$

where

$$M_{OUTmax} = \frac{3\pi(1+\sqrt{3})}{\sqrt{2(\pi^2+144)}} \approx 1.4678. \quad (58)$$

This condition bounds the output voltage region where previously derived results are valid.

III. THE EXACT SOLUTION

Essential step in obtaining the closed form solution is to establish symmetry relations between the input currents of the diode bridges. There are six of these currents, and each of them exhibits two zero crossings during the line period. Each of the zero crossings causes commutation in the corresponding leg of the diode bridge, where conducting is switched from one diode to another. There are twelve of these transitions during the line period. Symmetry in the rectifier operation forces the intervals between two adjacent zero crossings to be the same, resulting in twelve intervals of the duration of $\pi/6$ in the phase angle in which the rectifier is represented by an equivalent linear circuit.

The symmetries are caused both by the rectifier construction and by symmetry in the input voltage system. The first of the symmetries expresses waveforms of two of the input currents as phase shifted waveform of the third one

$$j_1(\varphi) = j_2\left(\varphi + \frac{2\pi}{3}\right) = j_3\left(\varphi + \frac{4\pi}{3}\right). \quad (59)$$

The second of the symmetries is an odd type symmetry of the input current during its half-period

$$j_k(\varphi) = -j_k(\varphi - \pi) \quad (60)$$

for $k \in \{1, 2, 3\}$. With these two symmetries, regarding signs of the currents the line period is divided into six segments of equal duration, $\pi/3$ in phase angle, as shown in [7].

Applying (59) in (1) expressed in the domain of complex Fourier coefficients and applying the time shifting theorem, the complex Fourier series coefficients of the expansion of i_{A1} are obtained as

$$\underline{I}_{A1n} = \frac{1 - pe^{-j\frac{2\pi}{3}n}}{p+2} \underline{I}_{1n} \quad (61)$$

while the coefficients for i_{B1} are obtained as

$$\underline{I}_{B1n} = \frac{p+1 + pe^{-j\frac{2\pi}{3}n}}{p+2} \underline{I}_{1n}. \quad (62)$$

Since

$$\frac{1 - pe^{-j\frac{2\pi}{3}n}}{p+2} e^{-j\frac{\pi}{6}n} - \frac{p+1 + pe^{-j\frac{2\pi}{3}n}}{p+2} = 0 \quad (63)$$

for $12n \pm 1$, where according to (42) the input currents contain nonzero harmonic components, currents i_{A1} and i_{B1} are related such that

$$i_{B1}(t) = i_{A1}\left(t - \frac{T}{12}\right) \quad (64)$$

where T is the line period. This result can be generalized to other output currents of the line-side interphase transformer, and expressed in terms of normalized variables as

$$j_{Bk}(\varphi) = j_{Ak}\left(\varphi - \frac{\pi}{6}\right). \quad (65)$$

In this manner, the line period is divided in twelve segments of $\pi/6$ in phase angle where the diode states remain unchanged, and the rectifier may be represented by an equivalent linear circuit. Besides, all of the line-side interphase transformer output currents i_{Ak} and i_{Bk} have the same shape, being different only in the phase displacement.

To obtain the exact solution, let us define θ as the phase angle where current i_{Ak} exhibits rising zero crossing,

$$j_{A1}(\theta) = 0, j_{A1}(\theta^-) < 0, j_{A1}(\theta^+) > 0. \quad (66)$$

In sinusoidal approximation, the angle θ is related to the phase lagging of the input currents ϕ as

$$\theta = \phi - \frac{\pi}{12}. \quad (67)$$

Next, let us define J_0 as

$$J_0 = j_1(\theta). \quad (68)$$

Starting from the initial value J_0 , the waveform of j_1 is according to (16) given by

$$\begin{aligned} j_1(\varphi) &= J_0 + \int_{\theta}^{\varphi} (m_1(\varphi) - m_{T1}(\varphi)) d\varphi = \\ &= J_0 + \cos\theta - \cos\varphi - \int_{\theta}^{\varphi} m_{T1}(\varphi) d\varphi. \end{aligned} \quad (69)$$

The integral of m_{T1} is determined according to the staircase waveform of Fig. 3.

Let us define values of j_1 at state changing instants during one half period as

$$J_l = j_1\left(\theta + l\frac{\pi}{6}\right) \quad (70)$$

for $l \in \{0, 1, 2, 3, 4, 5\}$. The values of J_l for $l > 0$ are determined as

$$J_1 = J_0 + \cos \theta - \cos \left(\theta + \frac{\pi}{6} \right) \quad (71)$$

$$J_2 = J_0 + \cos \theta - \cos \left(\theta + \frac{\pi}{3} \right) - \frac{\pi}{18} M_{OUT} \quad (72)$$

$$J_3 = J_0 + \cos \theta - \cos \left(\theta + \frac{\pi}{2} \right) - \left(1 + \sqrt{3} \right) \frac{\pi}{18} M_{OUT} \quad (73)$$

$$J_4 = J_0 + \cos \theta - \cos \left(\theta + \frac{2\pi}{3} \right) - \left(3 + \sqrt{3} \right) \frac{\pi}{18} M_{OUT} \quad (74)$$

and

$$J_5 = J_0 + \cos \theta - \cos \left(\theta + \frac{5\pi}{6} \right) - \left(3 + 2\sqrt{3} \right) \frac{\pi}{18} M_{OUT}. \quad (75)$$

Remaining values of the input current at the state transition points are determined applying symmetry (60). Besides, there is linear dependence between the values (71)–(75), again due to the symmetry.

At this point, values of θ and J_0 are not determined. To determine these parameters,

$$j_{A1}(\theta) = 0 \quad (76)$$

and

$$j_{B1} \left(\theta + \frac{\pi}{6} \right) = 0 \quad (77)$$

are used. Multiplying (1) and (4) with $p + 2$ and taking appropriate values of j_2 according to (59) and (60), the system to determine θ and J_0 is obtained as

$$J_0 + pJ_2 = 0 \quad (78)$$

and

$$(p + 1)J_1 - pJ_3 = 0. \quad (79)$$

The system of (78) and (79) reduces to

$$\begin{aligned} (\sqrt{3} - 1) \cos \theta + (3 - \sqrt{3}) \sin \theta + 2(\sqrt{3} + 1) J_0 &= \\ &= \frac{\pi}{9} (\sqrt{3} - 1) M_{OUT} \end{aligned} \quad (80)$$

and

$$(1 - \sqrt{3}) \cos \theta + (3 - \sqrt{3}) \sin \theta + 4J_0 = -\frac{2\pi}{9} M_{OUT}. \quad (81)$$

Solution of the system is

$$\theta = \frac{5\pi}{12} - \arcsin \left(\frac{\pi(\sqrt{2} + \sqrt{6})}{18} M_{OUT} \right) \quad (82)$$

and

$$J_0 = \frac{\sqrt{2} - \sqrt{6}}{4} \sqrt{1 - (2 + \sqrt{3}) \left(\frac{\pi M_{OUT}}{9} \right)^2} \quad (83)$$

which determines the rectifier input currents according to (69), (59) and (60). The waveform of $j_1(\varphi)$ during the half period $\theta < \varphi < \theta + \pi$ is obtained in a general form

$$j_1(\varphi) = M_{OUT} (\pi a - b(\varphi + \alpha)) - \cos \varphi \quad (84)$$

TABLE II
VALUES FOR PARAMETERS a AND b

interval	a	b
$\theta < \varphi < \theta + \frac{\pi}{6}$	$\frac{2+\sqrt{3}}{18}$	0
$\theta + \frac{\pi}{6} < \varphi < \theta + \frac{\pi}{3}$	$\frac{11+2\sqrt{3}}{36}$	$\frac{1}{3}$
$\theta + \frac{\pi}{3} < \varphi < \theta + \frac{\pi}{2}$	$\frac{11\sqrt{3}+2}{36}$	$\frac{\sqrt{3}}{3}$
$\theta + \frac{\pi}{2} < \varphi < \theta + \frac{2\pi}{3}$	$\frac{2}{3}$	$\frac{2}{3}$
$\theta + \frac{2\pi}{3} < \varphi < \theta + \frac{5\pi}{6}$	$\frac{13\sqrt{3}-2}{36}$	$\frac{\sqrt{3}}{3}$
$\theta + \frac{5\pi}{6} < \varphi < \theta + \pi$	$\frac{13-2\sqrt{3}}{36}$	$\frac{1}{3}$

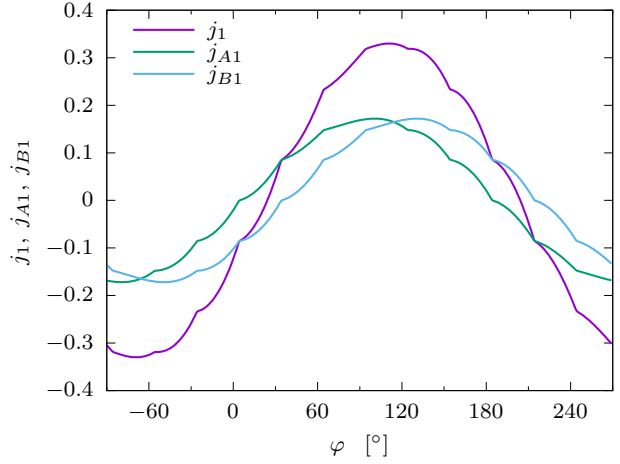


Fig. 5. Waveforms of j_1 , j_{A1} , and j_{B1} for $M_{OUT} = 1.4$.

where

$$\alpha = \arcsin \left(\frac{\pi(\sqrt{2} + \sqrt{6})}{18} M_{OUT} \right) \quad (85)$$

and values for parameters a and b depend on the phase angle segment, as given in Table II. Input currents of the diode bridges are determined as the output currents of the line-side interphase transformer according to (1)–(6). Waveforms of j_1 , j_{A1} , and j_{B1} obtained for $M_{OUT} = 1.4$ are shown in Fig. 5.

After the waveforms of the input currents are determined, their rms value is obtained as

$$J_{RMS} = \frac{\sqrt{3}}{54} \sqrt{486 + \left((6\sqrt{3} + 11) \pi^2 - 432 \right) M_{OUT}^2} \quad (86)$$

while the amplitude of the fundamental harmonic is obtained as

$$J_{m1} = \sqrt{1 - \left(\frac{8}{9} - \frac{16}{\pi^2} (2 - \sqrt{3}) \right) M_{OUT}^2} \quad (87)$$

which is close to the value obtained applying sinusoidal approximation (44).

After the rms value and the fundamental harmonic of the input current are determined, the total harmonic distortion of the input current is obtained from

$$THD = \frac{\sqrt{2J_{RMS}^2 - J_{m1}^2}}{J_{m1}} \quad (88)$$

which reduces to

$$THD = M_{OUT} \sqrt{\frac{(6\sqrt{3} + 11) \pi^4 + 7776\sqrt{3} - 15552}{486\pi^2 - 432(\pi^2 + 18\sqrt{3} - 36) M_{OUT}^2}}. \quad (89)$$

This value cannot be predicted applying sinusoidal approximation.

To determine the output current, symmetry properties (59), (60), and (65) are used, reducing the output current computation to

$$J_{OUT} = \frac{3}{\pi} \int_{\theta}^{\theta+\pi} j_{A1}(\varphi) d\varphi \quad (90)$$

which provides

$$\begin{aligned} J_{OUT} &= \frac{3(\sqrt{6} - \sqrt{2})}{\pi} \sqrt{1 - (2 + \sqrt{3}) \left(\frac{\pi M_{OUT}}{9}\right)^2} \\ &\approx 0.9886 \sqrt{1 - 0.4547 M_{OUT}^2}. \end{aligned} \quad (91)$$

In practice, it is convenient to have the inverted form of (91)

$$\begin{aligned} M_{OUT} &= \frac{9(\sqrt{6} - \sqrt{2})}{2\pi} \sqrt{1 - (2 + \sqrt{3}) \left(\frac{\pi J_{OUT}}{6}\right)^2} \\ &\approx 1.4829 \sqrt{1 - 1.0232 J_{OUT}^2}. \end{aligned} \quad (92)$$

Relations (91) and (92) are close to the results (47) and (48) obtained applying sinusoidal approximation, and have the same computational complexity. Actually, both of the solutions have the same form, while the parameters are slightly different. Besides, both of the methods provide the same solution for $M_{OUT} = 0$, where the higher order harmonics are absent from the system.

The output power of the rectifier in normalized form is given by

$$P_{OUT} = \frac{3(\sqrt{6} - \sqrt{2})}{\pi} M_{OUT} \sqrt{1 - (2 + \sqrt{3}) \left(\frac{\pi M_{OUT}}{9}\right)^2} \quad (93)$$

which reaches maximum for

$$\frac{dP_{OUT}}{dM_{OUT}} = 0 \quad (94)$$

at

$$M_{OUT} = \frac{9}{2\pi} (\sqrt{3} - 1) \approx 1.0486. \quad (95)$$

Normalized value of the maximum of the output power is

$$P_{OUTmax} = \frac{27}{\pi^2} (2 - \sqrt{3}) \approx 0.7330 \quad (96)$$

which is slightly lower than the value (52) predicted applying sinusoidal approximation.

In the case of the exact solution, where the higher order harmonics of the input currents are not neglected, the displacement power factor and the power factor differ. The power factor is obtained from

$$PF = \frac{\sqrt{2} P_{OUT}}{3 J_{RMS}} \quad (97)$$

which reduces to

$$\begin{aligned} PF &= \frac{4(3 - \sqrt{3})}{\pi} M_{OUT} \times \\ &\times \sqrt{\frac{81 - (2 + \sqrt{3}) \pi^2 M_{OUT}^2}{(\pi^2 (6\sqrt{3} + 11) - 432) M_{OUT}^2 + 486}}. \end{aligned} \quad (98)$$

The displacement power factor is obtained from

$$DPF = \frac{2 P_{OUT}}{3 J_{m1}} \quad (99)$$

which reduces to

$$\begin{aligned} DPF &= \frac{2(\sqrt{6} - \sqrt{2})}{3} M_{OUT} \times \\ &\times \sqrt{\frac{81 - (2 + \sqrt{3}) \pi^2 M_{OUT}^2}{9\pi^2 - 8(\pi^2 - 18(2 - \sqrt{3})) M_{OUT}^2}}. \end{aligned} \quad (100)$$

Due to the low THD of the input currents, the difference between (98) and (100) is small.

Boundary of the continuous conduction mode is determined in the same manner as in the case when the sinusoidal approximation was applied. When each of the diode bridge input currents crosses zero, causing commutation in the bridge, the current should keep its slope. Twelve such conditions may be written, and due to symmetry all of them provide the same result. In the case of the rising zero crossing of i_{A1} the condition is

$$\left. \frac{dj_{A1}}{d\varphi} \right|_{\varphi=\theta^+} > 0. \quad (101)$$

Since

$$\frac{dj_{A1}}{d\varphi} = \frac{1}{p+2} \frac{dj_1}{d\varphi} - \frac{p}{p+2} \frac{dj_2}{d\varphi} \quad (102)$$

according to (16) the slope of the normalized current is expressed in terms of the normalized voltages as

$$\frac{dj_{A1}}{d\varphi} = \frac{1}{p+2} (m_1 - m_{T1}) - \frac{p}{p+2} (m_2 - m_{T2}). \quad (103)$$

At the critical point of $\varphi = \theta^+$

$$\begin{aligned} \left. \frac{dj_{A1}}{d\varphi} \right|_{\varphi=\theta^+} &= \frac{1}{p+2} (m_1(\theta) - m_{T1}(\theta^+)) - \\ &- \frac{p}{p+2} (m_2(\theta) - m_{T2}(\theta^+)) \end{aligned} \quad (104)$$

which reduces to

$$\left. \frac{dj_{A1}}{d\varphi} \right|_{\varphi=\theta^+} = \frac{1}{p+2} \sin \theta - \frac{p}{p+2} \left(\sin \left(\theta - \frac{2\pi}{3} \right) + \frac{\sqrt{3}}{3} \right). \quad (105)$$

Finally, from (105) the criterion is obtained as

$$M_{OUT} < M_{OUTmax} \quad (106)$$

where

$$M_{OUTmax} = \frac{9}{\sqrt{\pi^2 (2 + \sqrt{3}) - 9\sqrt{3} + 18}} \approx 1.4366 \quad (107)$$

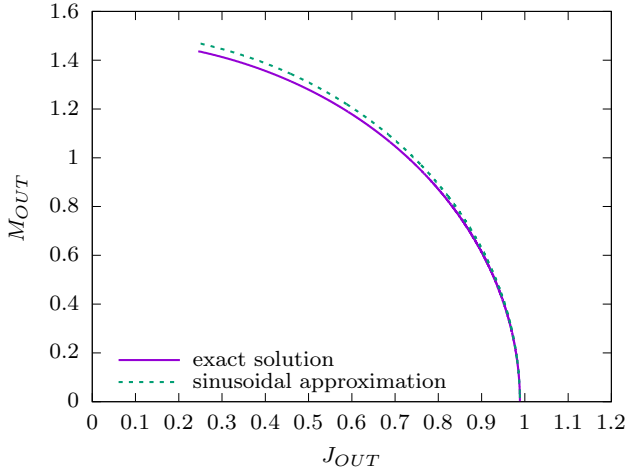


Fig. 6. Dependence of M_{OUT} on J_{OUT} .

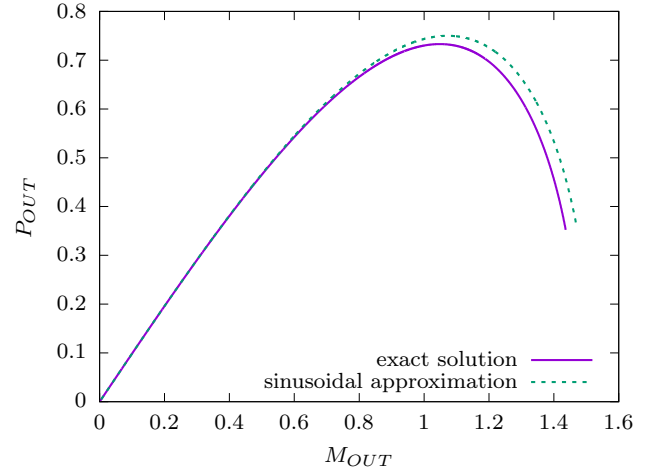


Fig. 7. Dependence of P_{OUT} on M_{OUT} .

which is close to the value (58) obtained applying the sinusoidal approximation, but somewhat lower. The same result is obtained from the condition

$$\left. \frac{dj_{B1}}{d\varphi} \right|_{\varphi=\pi/6+\theta^+} > 0 \quad (108)$$

as well as the remaining ten zero crossing cases during the line period.

IV. COMPARISON OF THE SOLUTIONS

To compare the solutions, the diagrams that predict relevant performance parameters of the rectifier are plotted. The first of the diagrams relates the output voltage and the output current. The diagram is plotted in Fig. 6 for the rectifier operating in the continuous conduction mode. The curves indicate good agreement between the solutions in the area of low output voltages, where the input currents are less polluted by the higher order harmonics. Sinusoidal approximation predicted higher output current than the exact solution, which is the effect also observed in [7]. However, due to the twelve-pulse nature of m_{Tk} voltages containing lower amount of higher order harmonics than corresponding six-pulse waveforms of [7], agreement between the curves is better than in [7].

Dependence of the output power on the output voltage is plotted in Fig. 7. Again, agreement between the curves is good for low output voltages, with lower distortion of the input currents. Both of the curves expose maxima predicted by (52) and (96). Somewhat wider operation range for the continuous conduction mode predicted by the sinusoidal approximation can be observed. Sinusoidal approximation also predicted somewhat larger maximum of the output power.

Dependence of the power factor on the output voltage is presented in Fig. 8. The power factor and the displacement power factor obtained applying the sinusoidal approximation (53) are presented in dashed line, while the exact value of the power factor is presented in solid line. The difference between the curves can barely be noticed, except in the area where predicted ranges of the continuous conduction mode are different. To provide better illustration, difference between

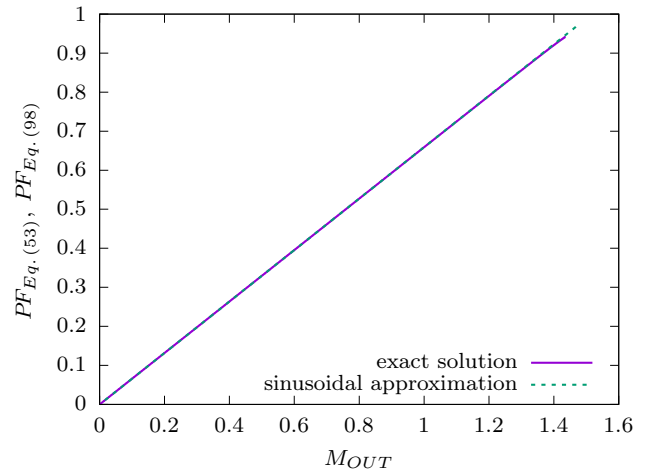


Fig. 8. Power factor.

the power factor obtained applying sinusoidal approximation and the exact solution in the area where the exact solution predicts the continuous conduction mode is presented in Fig. 9 in dashed line. The difference is lower than 0.5%, being the highest at the boundary between the continuous and the discontinuous conduction mode. In the same figure the difference between the displacement power factor and the power factor, both resulting from the exact solution, is presented in solid line. The difference between the displacement power factor and the power factor is low, lower than 0.1%, due to the low harmonic pollution of the input currents.

Sinusoidal approximation cannot predict distortion of the input currents. Total harmonic distortion obtained by the exact solution is plotted in Fig. 10. In the whole range of the output voltage where the converter operates in the continuous conduction mode, the input current THD is lower than 4.02%, which is less than in the case of the six-pulse rectifier analyzed in [7]. The same as in [7], the input current THD is smaller for lower values of the output voltage.

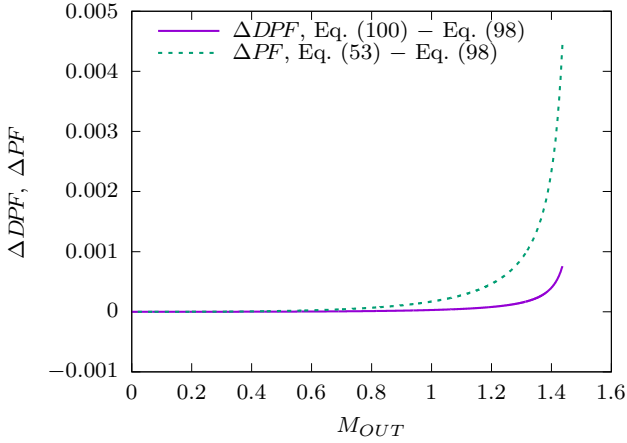


Fig. 9. Difference from the power factor.

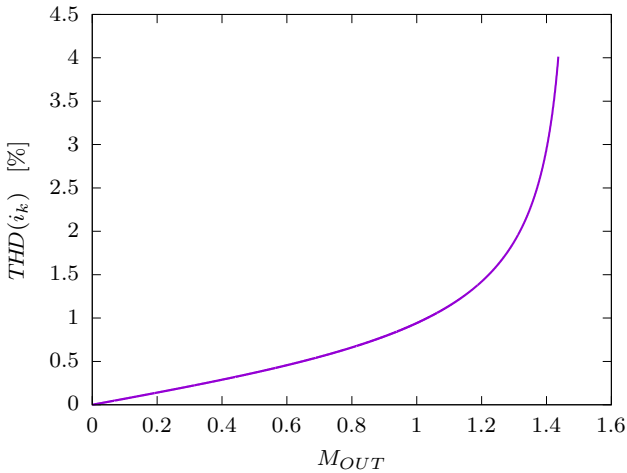


Fig. 10. Dependence of the input current THD on the output voltage.

V. CONCLUSION

In this paper, analysis of a three-phase twelve-pulse output voltage type rectifier is performed applying sinusoidal approximation and the exact analytical approach. The sinusoidal approximation, besides providing the approximate solution, proved to be useful in improving understanding of the rectifier operation and preparing ground for the exact analysis, providing directly applicable intermediate results regarding the rectifier voltage waveforms. The exact solution is based on symmetry properties of the input currents and the line-side interphase transformer output currents. It is shown that the three-phase voltages and currents, besides common phase shifting symmetry over one third of the line period and the odd type waveform symmetry over one half of the line period, has another symmetry property that corresponding output currents of the line-side interphase transformer are mutually shifted for one twelfth of the line period. This causes the line-side interphase transformer output currents to cross zero in regular intervals of $\pi/6$ in phase angle causing diode state changes. Except for the phase displacement, this causes shape of the line-side interphase transformer input voltages to be

the same as in the analysis performed applying sinusoidal approximation.

After the waveforms of the line-side interphase transformer input voltages are known, waveforms of the input currents are obtained integrating the inductor voltages for an assumed value of the output voltage. Due to the symmetry properties, it was sufficient to determine waveform of one of the phase currents over one half of the line period. To completely determine analytical description of the input current waveform, two parameters remained to be determined: phase delay of the line-side interphase transformer input voltage with regard to the corresponding phase voltage and the value of the corresponding input current at a diode state changing instant, i.e. the constant of integration. These two parameters are obtained from an equation system that imposes the line-side interphase transformer output currents to have zero crossings at appropriate phase angles.

When the analytical description of the input currents is determined, closed form expressions for their rms value and the fundamental harmonic amplitude are obtained. These two parameters enable computation of the input current THD, which is a parameter that cannot be predicted applying the sinusoidal approximation. The exact solution provided a closed form expression for the THD, indicating that in the whole region of the output voltage where the rectifier operates in the continuous conduction mode the input current THD is lower than about 4%. Dependence of the output current on the output voltage is determined next. Resulting expression is slightly different from the expression obtained applying the sinusoidal approximation, but both of them have the same computational complexity. Value of the output current enables computation of the output power, the power factor, and the displacement power factor. In the output current and the output power, the sinusoidal approximation predicted somewhat higher values than the exact solution. In the power factor and the displacement power factor, the difference between the results is negligible.

REFERENCES

- [1] M. Depenbrock, C. Niermann, "A new 12-pulse rectifier with line-side interphase transformer and nearly sinusoidal line currents," *Proceedings of the Power Electronics and Motion Control Conference*, Budapest, 1990, pp. 374–378.
- [2] C. Niermann, "New rectifier circuits with low mains pollution and additional low cost inverter for energy recovery," *Proceedings of the European Power Electronics Conference*, Aachen, 1989, pp. 1131–1136.
- [3] M. Depenbrock, C. Niermann, "A new 18-pulse rectifier circuit with line-side interphase transformer and nearly sinusoidal line currents," *Proceedings of the 2nd International Power Electronics Conference (IPEC)*, Tokyo, 1990, pp. 539–546.
- [4] P. Mysiak, "A 24-pulse diode rectifier with coupled three-phase reactor," *Journal of the Chinese Institute of Engineers*, vol. 30, No. 7, pp. 1197–1212, 2007.
- [5] K. Oguchi, G. Maeda, N. Hoshi, T. Kubota, "Coupling rectifier systems with harmonic cancelling reactors," *IEEE Industry Applications Magazine*, vol. 7, no. 4, pp. 53–63, July/Aug. 2001.
- [6] V. Caliskan, D. J. Perreault, T. M. Jahns, and J. G. Kassakian, "Analysis of three-phase rectifiers with constant-voltage loads," *IEEE Transactions on Circuits and Systems I, Fundamental Theory and Applications*, vol. 50, no. 9, pp. 1220–1226, Sep. 2003.
- [7] P. Pejović, J. W. Kolar, "Exact analysis of three-phase rectifiers with constant voltage loads," *IEEE Transactions on Circuits and Systems-II: Express Briefs*, vol. 55, no. 8, pp. 743–747, Aug. 2008.